Available online at www.sciencedirect.com
SCIENCE DIRECT®
C. R. Chimie 8 (2005) 369–378
COMPTES RENDUS CHIMIE
http://france.elsevier.com/direct/CRAS2C/

Full paper / Mémoire

A new synthesis method for the preparation of ITQ-7 zeolites and the characterisation of the resulting materials

Sandra Leiva, Maria José Sabater, Susana Valencia, German Sastre, Vicente Fornés, Fernando Rey *, Avelino Corma

Instituto de Tecnología Química (CSIC–UPV), Avenida de los Naranjos, s/n, 46022 Valencia, Spain

Received 5 July 2004; accepted 13 January 2005

Available online 14 March 2005

Abstract

A new and convenient synthesis procedure for the preparation of ITQ-7 within a wide range of compositions is described. The most relevant feature of this new method is that it has allowed to obtain the pure silica ITQ-7 zeolite that was not possible to synthesise since the earliest structure directing agent (SDA) reported for the synthesis of this material [L.A. Villaescusa, P.A. Barrett, M.A. Camblor, Angew. Chem. Int. Ed. 38 (1999) 1997] was discontinued from the commercial suppliers. The new SDA is *N*-butyl-*N*-cyclohexyl-pyrrolidinium cation that can be easily prepared through a reductive amination of ketones reaction followed by quaternisation of the resulting amines. This new SDA has allowed to synthesise ITQ-7 zeolites, as pure silica materials, but also Al has been introduced in its framework, providing acid properties to the resulting solids. In this work, the synthesis procedure and characterisation of the resulting solids will be presented in detail and compared to the ITQ-7 zeolites obtained through synthesis procedures previously reported [L.A. Villaescusa, P.A. Barrett, M.A. Camblor, Angew. Chem. Int. Ed. Engl. 38 (1999) 1997; A. Cantín, A. Corma, M.J. Díaz-Cabañas, F. Rey, G. Sastre, Conf. Proc. 14th Int. Zeolite Conf., Cape Town, South Africa, 2004]. ***To cite this article: S. Leiva et al., C. R. Chimie 8 (2005)***.
© 2005 Académie des sciences. Published by Elsevier SAS. All rights reserved.

Résumé

Cet article décrit une voie de synthèse nouvelle et pratique de la zéolithe ITQ-7, dans une large gamme de compositions. La caractéristique la plus innovante de cette nouvelle méthode est la possibilité d'obtenir le matériau en silice pure, qui ne pouvait plus se préparer depuis que l'agent directeur de structure (SDA) décrit pour cette synthèse n'était plus disponible dans le commerce. Ainsi, le nouveau template employé est le cation *N*-cyclohexyl-pyrrolidinium, qui peut être facilement obtenu par amination réductive de cétones, suivie d'une quaternisation de l'amine obtenue. Ce nouveau SDA a permis la synthèse de zéolithes ITQ-7, non seulement en silice pure, mais aussi contenant dans leur structure de l'aluminium, qui confère ainsi des propriétés acides au matériau obtenu. Par ailleurs, ce travail présente en détail les procédures de synthèse et les résultats de la caractérisation des différents solides obtenus, ceux-ci étant comparés à ceux déjà décrits dans la littérature [L.A. Villaescusa, P.A. Barrett, M.A. Camblor, Angew. Chem. Int. Ed. 38 (1999) 1997; A. Cantín, A. Corma, M.J. Díaz-Cabañas, F. Rey, G. Sastre, Conf. Proc. 14th Int. Zeolite Conf., Cape Town, South Africa, 2004]. ***Pour citer cet article : S. Leiva et al., C. R. Chimie 8 (2005)***.
© 2005 Académie des sciences. Published by Elsevier SAS. All rights reserved.

* Corresponding author.
E-mail address: frey@itq.upv.es (F. Rey).

1631-0748/$ - see front matter © 2005 Académie des sciences. Published by Elsevier SAS. All rights reserved.
doi:10.1016/j.crci.2005.01.010

Keywords: Zeolite synthesis; NMR and IR spectroscopies; X-ray diffraction; Isomorphic Ge and Al substitution

Mots clés : Synthèse de zéolithes ; Spectroscopies RMN et infrarouge ; Diffraction de rayons X ; Substitution isomorphique par Ge et Al

1. Introduction

The success of zeolites in catalytic processes is based on the presence of pores with opening dimensions close to the molecular sizes as well as on high surface areas and pore volumes. This provides to these crystalline solids of high adsorption capacities and the ability to act as true molecular sieves. This main characteristic joined to the possibility of generating catalytically active sites; provide to the zeolite a wide area of applications in chemical processes of technological interest.

Considering the pore aperture of the zeolites, these are typically classified in small (8R), medium (10R), large (12R) and ultralarge (>12R) zeolites depending on the number of $TO_{4/2}$ that conform the channel window. Among them, zeolites having three-directional channel systems with large channel apertures are the most important, since they offer the lowest restriction to the reactants to reach the catalytic centres and to the products to diffuse out of the zeolite during the course of the reaction process.

The unique examples of tridirectional large pore zeolites were Faujasite and Beta zeolite until 1999 when ITQ-7 was reported [1]. Later, other tridirectional large pore zeolites have been obtained such as the polymorph C of the Beta zeolite [3,4] and ITQ-21 [5].

In the earliest communication on ITQ-7 [1], the authors only reported the synthesis of the pure silica zeolite and therefore, no catalytic applications were afforded. Later, it was found that Ti can be introduced in the pure silica materials, but in a very small amount, yielding to some catalytic activity [6]. Also, aluminium substituted ITQ-7 zeolites can be prepared through a two step synthesis procedure [7], consisting in preparing the B-ITQ-7 zeolite, which is exchanged by Al following the procedure of Lobo and Davis [8]. It was described that the incorporation of Ge strongly favours the crystallisation of ITQ-7 zeolites, allowing to introduce Al or Ti in framework position by direct synthesis [7,9] opening the possibility for a variety of catalytic processes, showing the benefit of its tridirectional large pore system [10–13]. The stabilisation effect of the ITQ-7 framework when Ge is incorporated into the synthesis and the preferential location of Ge in the Double Four Ring Units (D4R) of ITQ-7 zeolite were studied in detail by a large suite of characterisation techniques in combination with theoretical ab initio calculations [14].

However, since these studies, no more reports on ITQ-7 have been reported may be due to the fact that the starting amine used for the preparation of ITQ-7 zeolite was discontinued for the commercial suppliers. Only very recently, it has been reported a new synthesis of ITQ-7 using a structure directing agent (SDA) obtained by a Diels–Alder reactions which has allowed to prepare Ge-containing zeolites, but not the pure silica ITQ-7 material [2].

Here, we report the synthesis of ITQ-7 zeolites using *N*-butyl-*N*-cyclohexyl-pyrrolidine cations as SDA that has allowed to obtain ITQ-7 zeolites in a very wide range of chemical compositions, including the pure silica zeolite.

2. Experimental

2.1. Synthesis of the organic SDA

The synthesis route followed to obtain the SDAs was the versatile reductive amination of ketones using the cyclohexanone as ketone and pyrrolidine as secondary amine. This reaction yields the corresponding enamine, which is reduced with sodium cyanoborohydride to the final tertiary amine in one-pot synthesis step. Finally, the quaternisation of the resulting *N*-cyclohexyl-pyrrolidine was carried out by reacting with butyl iodide. The reaction scheme of the synthesis of SDAs prepared in this work is presented in Fig. 1.

A solution of 44.6 g (638 mmol) of pyrrolidine, 50 ml of 5 N HCl–methanol, 10.0 g (102 mmol) of cyclohex-

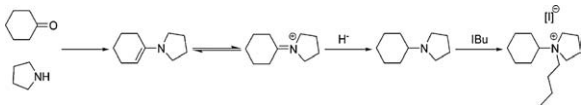

Fig. 1. Scheme of the synthesis of *N*-butyl-*N*-cyclohexyl-pyrrolidium iodide.

anone and 5.1 g (81 mmol) of $NaBH_3CN$ in 200 ml of methanol was prepared. The resulting solution was stirred for 72 h, then concentrated HCl was added until pH < 2 and the methanol was removed in vacuum. The residue was taken up in 100 ml of water and extracted with three 200 ml portions of diethyl ether. The aqueous solution was brought to pH 10 with KOH, saturated with NaCl and extracted with three 100 ml portions of diethyl ether. The organic extract was dried ($MgSO_4$) and evaporated in vacuum.

The last step for the synthesis of the SDA is the quaternisation of the resulting *N*-cyclohexyl-pyrrolidine with butyl-iodide as follows:

- 15.3 g of *N*-cyclohexyl-pyrrolidine (100 mmol) and 46.0 g (250 mmol) of butyl iodide were added in a 250 ml round bottom flask. The reaction mixture was stirred at 100 °C for 4 days. Then, approximately 300 ml of acetone were added on the resulting reaction product, and the solid was precipitated with diethyl ether. Finally, the needed purity of the solid was achieved by subsequent re-crystallisation with acetone and diethyl ether. This synthesis affords 23.6 g (70% yield) of the final product.

The final *N*-butyl-*N*-cyclohexyl-pyrrolidinium iodide salt was characterised by means of elemental analysis, ^{13}C- and ^{1}H-NMR spectroscopies indicating that the purity was close to 100%.

The organic SDA was exchanged into the hydroxide form with an anionic resin (Amberlite IRN-78). The exchange yields were always close to 100% (below the detection limit of a iodide selective electrode) and the corresponding aqueous solutions were titrated and used as SDA^+ and OH^- sources in the synthesis of ITQ-7 zeolites.

2.2. Synthesis of ITQ-7 zeolite

The synthesis gels used in this work have the following general molar composition:

$$(1-x)\ SiO_2 :\ x\ GeO_2 :\ y\ Al_2O_3 :\ 0.54\ SDAOH :\ 0.54\ HF :\ z\ NH_4F :\ w\ H_2O$$

The appropriate amounts of tetraetylorthosilicate (TEOS), GeO_2 and triisopropylaluminium (TIPA, when required) were added to the SDAOH solution and stirred until a homogeneous gel was formed. The TEOS and TIPA were hydrolysed and the alcohol was evaporated. The water content was adjusted to reach the final gel composition, and finally the appropriate amounts of HF and NH_4F were added to the reaction mixture. The resulting thick gel was manually homogenised. Subsequently, the zeolite crystallisation was carried out at the autogenous pressure at different temperatures in Teflon lined stainless steel autoclaves for different crystallisation times. The solids were recovered by filtration and exhaustively washed with distilled water and acetone and finally dried at 100 °C, overnight.

2.3. Physico-chemical characterisation techniques

Phase selectivity and crystallinity were determined by X-ray powder diffraction data, recorded in a Philips X'Pert Pro diffractometer equipped with an X'Celerator detector, using the Cu Kα radiation provided with fixed divergence (1/8°) and anti-scatter (1/4°) slits.

Ge and Al were analysed with a Varian SpectraAA-10Plus and the standard deviations obtained for samples with a well known Ge or Al contents were below 5%. N, C and H contents were determined with a Carlo Erba 1106 elemental organic analyser.

The crystal size and morphology were monitored by scanning electron microscopy (SEM) using a JEOL JSM-6300 microscope.

The IR spectra (Nicolet 710 FTIR spectrometer) in the region of framework vibrations were recorded using the KBr pellet technique. Acidity measurements of calcined Al-containing ITQ-7 were carried out on wafers of 10 mg cm^{-2} previously outgassed at 400 °C and 10-3 Pa for 16 h. Then, 660 Pa of pyridine were introduced into the IR cell at room temperature. After equilibrium, the ITQ-7 sample was stepwise outgassed at 150, 250 and 350 °C under vacuum, and the IR spectra in the hydroxyl (4000–3300 cm^{-1}) and C–C (1750–1350 cm^{-1}) stretching regions were recorded at room temperature. N_2 and Ar isotherms were obtained in an ASAP 2010 Micromeritics apparatus.

^{19}F- solid state NMR spectra were recorded under magic angle spinning (MAS) at ambient temperature with a Bruker AV-400-WB spectrometer at 376.3 MHz. The ^{19}F chemical shifts were referred to $CFCl_3$. A recycle delay of 80 s was used to ensure the complete recovery of the ^{19}F magnetisation with pulses of 5 ms corresponding to a magnetisation flip angle of π/2, and spinning rates of c.a. 16–17 kHz.

3. Results and discussion

3.1. Effect of the synthesis conditions on phase selectivity

The *N*-butyl-*N*-cyclohexyl-pyrrolidium cation (BCHP) was essayed as SDA in the synthesis of pure silica and silica–alumina zeolites at nearly neutral pH using fluoride as mobilising agent. The synthesis conditions used in this work and the observed phase selectivities are given in Table 1.

It is observed that this SDA mostly drives the syntheses towards Beta and ZSM-11 (MEL) zeolites. In pure silica Beta zeolite is the main product when the synthesis is carried out at low temperature and short crystallisation times. Then, as expected from the Ostwald ripening rule [15], pure silica Beta zeolite is transformed in ZSM-11 zeolite, that possesses a higher framework density. Notoriously, Beta formation is greatly disfavoured when Al is incorporated into the synthesis gel, and in these cases, mostly ZSM-11 is the phase formed.

The elemental analyses and ^{13}C-CP-MAS-NMR spectra indicate that the SDA remains intact inside of the zeolites even after long crystallisation times.

Additionally to ZSM-11 and Beta zeolite, also ITQ-7 (ISV) was detected at relatively short crystallisation times, low synthesis temperature and in diluted gels, indicating that this SDA can also be fitted inside the ITQ-7 zeolite. In addition to this result we had reported that the presence of Ge strongly favours the formation of ITQ-7 zeolites [14]. This moved us to introduce Ge into the synthesis media. Table 2 reports the observed phase selectivity for Ge-containing synthesis using the *N*-butyl-*N*-cyclohexyl-pyrrolidine as SDA in fluoride media (Table 2).

The presence of Ge dramatically changes the phase selectivity and the only product observed in the whole range of gel compositions essayed in this work was ITQ-7. This is a clear prove of the directing effect of Ge towards zeolite structures that contain D4R units in their frameworks. Indeed, neither MEL nor Beta contain such cage in their structures, but ITQ-7 does.

The high stability of ITQ-7 is also reflected on the stability of this structure after prolonged crystallisation times, contrarily to the expected from the Ostwald ripening rule in which low framework density zeolites are generally formed at prolonged crystallisation times.

Since, as it was discussed above, ITQ-7 phase was detected as pure silica material (see Table 1), we thought the possibility of increasing the crystallisation rate of the pure-silica and the Al-containing ITQ-7 zeolites by seeding with Ge-ITQ-7. The results obtained by introducing 5% of the silica as seeds of Ge-ITQ-7 are shown in Table 3. There, it is observed that seeding with ITQ-7 strongly favours the growing of ISV structure for the pure silica material with respect the competing ZSM-11 phase. Indeed, essentially pure silica ITQ-7 zeolites were obtained in very short crystallisation times (3 days) (Table 3).

When the synthesis of Al containing ITQ-7 zeolites were attempted, the detected phase using the same synthesis conditions than above was ZSM-11, on the con-

Table 1
Effect of the gel concentration and Al content on the observed phase selectivity

H_2O/Si	Si/Al	Temperature (°C)	Time (days)	Phase
7.25	∞	150	12	MEL + ISV
			50	MEL
		175	14	MEL + β
			42	MEL
3	∞	150	6	β + MEL
			11	β + MEL
		175	4	MEL + β
			8	MEL + β
7.25	50	150	7	MEL
			33	MEL
		175	3	Amorphous
			10	MEL
3	50	150	3	MEL + β
			24	MEL
7.25	25	150	8	Amorphous
			18	MEL

Gel composition: SiO_2:*y* Al_2O_3:0.54 SDAOH:0.54 HF:*w* H_2O.

Table 2
Effect of the presence of Ge in the synthesis media on the observed phase selectivity

Si/Ge	(Si + Ge)/Al	Phase
5	∞	ISV
	50	ISV
	25	ISV
	15	ISV
10	∞	ISV
	50	ISV
∞	∞	β + MEL
	50	MEL

Synthesis conditions: Temperature = 175 °C; time = 7 days; (1 – *x*) SiO_2:*x* GeO_2:*y* Al_2O_3:0.54 SDAOH:0.54 HF:7.25 H_2O.

Table 3
Effect of seeding on the synthesis of Al-ITQ-7 zeolites

F/Si [a]	H_2O/Si [a]	Si/Al [a]	Phase
0.54	7.25	∞	ISV
			ISV [b]
		50	MEL
	3.00	50	MEL + ISV
2.00	7.25	50	ISV

Synthesis conditions: Temperature = 175 °C; time = 7 days; SiO_2:*y* Al_2O_3:0.54 SDAOH:0.54 HF:*z* NH_4F:*w* H_2O 5 wt.% of the silica was introduced as seeds of a Ge-ITQ-7 of Si/Ge = 6.

[a] The Ge introduced as consequence of the seeds is not consider in these ratios.

[b] ITQ-7 zeolite synthesised in the above row was used as seeds.

trary when the crystallisation was carried out in a more concentrated gel (H_2O/Si = 3), the low framework ISV structure was detected as a minor phase. Recently, we have proposed that the fluoride concentration, instead of the gel concentration, is the most important parameter in explaining the directing effect of Fluoride anions [16]. By applying this approach, we found that when the F/Si ratio is increased up to 2, ITQ-7 zeolite was obtained as a pure phase, but its chemical analysis shows that Al was not incorporated into the solid. This can be understood by considering that high fluoride and aluminium contents generate negatively charged silicates (fluorosilicates or aluminosilicates, respectively). Therefore, both species, F^- and Al^{3+}, compete for being compensated by the organic cations present in the synthesis media. Then, as the fluoride concentration increases, the aluminium has less chance to be incorporated into the zeolite framework.

3.2. Characterisation of the ITQ-7 materials

Representative ITQ-7 samples synthesised by this new method were studied in some detail. The most relevant characterisation results including XRD, IR, MAS-NMR spectroscopies and acid characterisation, will be discussed.

3.2.1. Germanium substituted ITQ-7 zeolites

The X-ray diffraction patterns of the ITQ-7 samples with different Ge contents are plotted in Fig. 2. Also, for comparison purposes the simulated XRD pattern for the pure silica ITQ-7 zeolite is presented [17] (Fig. 2).

It is observed that all the samples are highly crystalline and no extra-phases or amorphous material are

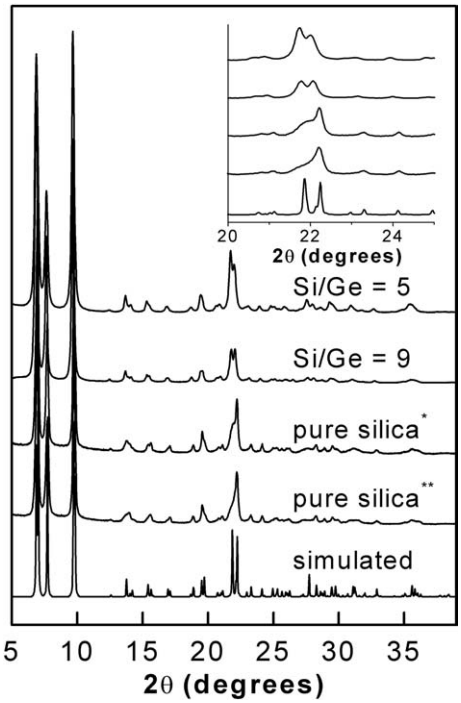

Fig. 2. XRD patterns of pure silica and Ge-containing ITQ-7 samples in the calcined state.
* Seeded with Ge-ITQ-7. ** Seeded with pure silica ITQ-7.

observed in the XRD patterns, indicating the purity of the Ge samples synthesised using BCHP as SDA. However, important differences in the relative intensities of some reflections were observed. Particularly, the intensity of XRD diffraction at 21.85° strongly decreases as the Ge content of the samples decreases (see inset of Fig. 2). This has been attributed to the presence of intergrowths [1,18] in the ITQ-7 materials and suggests that the level of intergrowth increases as the Ge loading decreases in the solid, being found the maximum level of intergrowth in the all-silica ITQ-7 sample prepared by seeding with pure silica zeolite.

The high crystallinity of the pure silica and Ge-containing ITQ-7 samples was also evidenced by the micropore volume and surface area determined from the N_2 adsorption isotherm using the *t*-plot method and the B.E.T. equations that were always closer to 0.24 $cm^3\ g^{-1}$ and 537 $m^2\ g^{-1}$, respectively.

The isomorphic substitution of Ge in the ITQ-7 framework was assessed by several physico-chemical techniques. The first evidence was obtained from the continuous shift of the X-ray reflections towards low 2θ angles as the Ge content increases in the ITQ-

7 sample. Indeed, the analyses of the XRD patterns allowed to calculate the unit cell volumes of the different calcined ITQ-7 samples, being found that there is a continuous expansion of the unit cell volume with the Ge content (Fig. 3).

This enlargement of the unit cell parameters with the Ge content can be attributed to the larger ionic radius of Ge compared to that of the silicon atoms.

The IR spectra of the as-prepared pure silica and Ge-containing ITQ-7 are presented in Fig. 4. There, it is observed that the ratio between the asymmetric modes of the stretching Si–O–Si vibration, that appear in the pure silica spectrum at 1098 and 1040 cm^{-1}, decreases as the Ge content increases. Also, new vibration bands at 1001 and 890 cm^{-1} appear as the Ge content increases. These bands were assigned to the stretching vibrations of Si–O–Ge species [14,18], supporting the conclusion that isomorphic substitution of Ge in framework positions is occurring (Fig. 4).

Finally, ^{19}F-MAS-NMR spectroscopy has been found as a powerful tool in localising Ge when is placed at singular T positions in D4R cages, where F^- anions tends to be located [4,5,14,20–22].

The ^{19}F-MAS-NMR spectra of the pure silica and Ge-containing ITQ-7 samples in the as-prepared form are presented in Fig. 5. The spectrum of the pure silica material presents a single resonance at –38.0 ppm, which is assigned to the presence of fluoride anions within the small D4R cage in a pure silica environment [23]. It should be noted that previous publications have

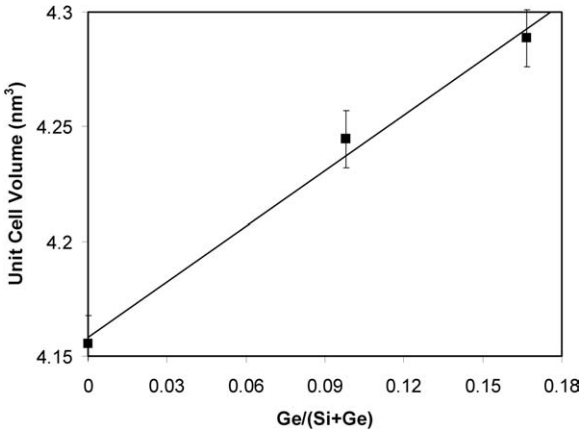

Fig. 3. Unit cell volume of calcined ITQ-7 samples versus Ge/(Ge + Si) ratio.

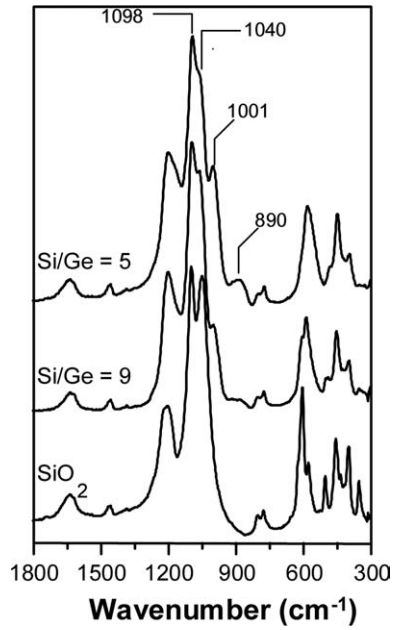

Fig. 4. Infrared spectra of the as-prepared pure silica and Ge-containing ITQ-7 zeolites.

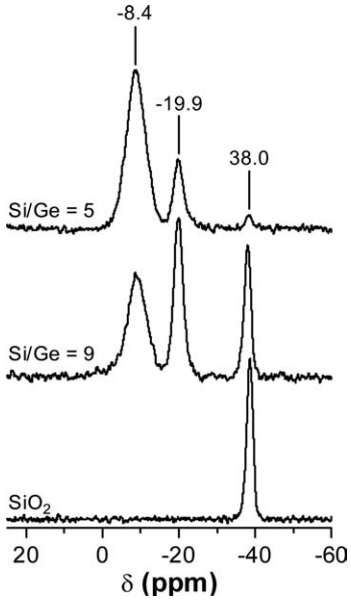

Fig. 5. ^{19}F-MAS-NMR spectra of pure silica and Ge-containing ITQ-7 zeolites.

reported the appearance of two resonances in the ^{19}F-MAS-NMR spectra of pure ITQ-7 materials corresponding to the presence of two non-equivalent D4R cages in the ITQ-7 structure [1,18]. In this work, we observe a single resonance that could be due to the high level of intergrowth of the pure silica sample studied here, when compared to those previously reported (Fig. 5).

The ^{19}F-MAS-NMR-spectra of the Ge-ITQ-7 samples show the appearance of two resonances at –19.9 and –8.4 ppm that grow up as the Ge content increases. These NMR signals have been assigned to fluoride anions located within D4R cages with different number of Ge atoms substituting Si sites [14,20]. Along our earlier work regarding to Ge location in D4R containing zeolites, the resonance at –19.9 ppm has been attributed to fluoride anions having one Ge and seven Si cations in its closer neighbouring, while the signal at –8.4 has been assigned to fluoride atoms within a D4R cage formed by three Ge and five silicon atoms [4,14,22]. Recently, Wang et al. [20] have reported a different assignation to these F-MAS-NMR signals when appeared in Ge-containing octadecasil samples. The resonance at –19.9 ppm was attributed to fluoride anion encapsulated within D4R cages formed by two Ge and six Si atoms, while the signal at –8.4 ppm was assigned to fluoride species entrapped in D4R cages containing four Ge and four Si cations.

Then, it is possible to calculate the averaged Si/Ge ratio in the D4R units in the ITQ-17 structure from the integrated intensities of the ^{19}F-NMR signals using both assignations. Also, by considering that Ge has a strong tendency to preferentially occupy the T sites placed at the D4R units, it is feasible to calculate the Si/Ge ratio of the zeolite by assuming that all Ge is placed at D4R sites [4,14,20]. When this is done the values given in Table 4 are obtained (Table 4).

It is clear that the Si/Ge ratios obtained from chemical analysis are much closer to those obtained by ^{19}F-MAS-NMR spectroscopy using the assignation for our earlier publication discussing the Ge location in ITQ-7 zeolites [14] than that reported for octadecasil samples [20]. Even more important, Ge selectively occupies those sites placed at D4R units, while the other sites remain as nearly pure siliceous. These results are in line with those previously reported for ITQ-7 [14], but also for many other Ge-containing zeolites having D4R in their structures, such as ITQ-17 [4], ITQ-21 [5] or ITQ-13 [21].

3.2.2. *Aluminium containing ITQ-7 zeolites*

As discussed in Section 3.1., ITQ-7 was successfully crystallised with aluminium containing gels (see Tables 2 and 3). This is clearly demonstrated by the XRD patterns of these samples shown in Fig. 6.

There, it is observed that the Al-ITQ-7 materials posses good crystallinities and there are no amorphous or extra-phases in the samples. The chemical analyses of the Al-ITQ-7 (Table 5) indicate that Ge is incorporated into the solid in nearly quantitative yields, but the Al contents in the solids were found to be much lower than those of the synthesis media, showing the difficulties in obtaining Al containing ITQ-7 zeolites (Table 5).

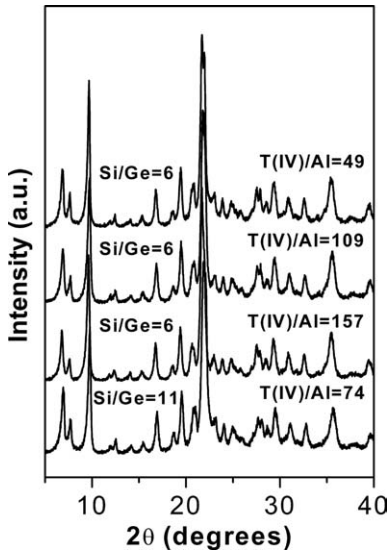

Fig. 6. XRD patterns of as-made Al-Ge-containing ITQ-7 zeolites.

Table 4
Si/Ge ratios of ITQ-7 zeolites determined by chemical analysis and ^{19}F-MAS-NMR spectroscopy

$(Si/Ge)_{gel}$	Chemical analysis	^{19}F-MAS-NMR (assignation as Ref. [14])		^{19}F-MAS-NMR (assignation as Ref. [20])	
	$(Si/Ge)_{zeolite}$	$(Si/Ge)_{D4R}$	$(Si/Ge)_{zeolite}$	$(Si/Ge)_{D4R}$	$(Si/Ge)_{zeolite}$
∞	n.d.	∞	∞	∞	∞
10	9	3.7	8.5	1.2	3.5
5	5	2.1	5.2	2.2	5.4

Table 5
Chemical composition of Ge-Al-ITQ-7 samples

Synthesis media		ITQ-7 zeolite	
Si/Ge	T(IV)/Al	Si/Ge	T(IV)/Al
∞ [a]	50 [a]	∞	∞
10	∞	9	∞
	50	11	74
5	∞	5	∞
	50	6	151
	25	6.5	108
	15	6	49

[a] Seeded with Ge-ITQ-7.

The isomorphic substitution of Al in Ge-ITQ-7 was proved, by means of ^{27}Al-MAS-NMR spectroscopy (Fig. 7), by the presence of a single resonance at –45 ppm assigned to tetrahedrally coordinated Aluminium in silica environments [24] (Fig. 7).

The acid properties of the Al-containing ITQ-7 zeolites were studied by means of the stepwise pyridine desorption technique followed by IR spectroscopy (Fig. 8).

The Al-Ge-ITQ-7 zeolite presents four bands in the stretching OH region (top spectrum of Fig. 8a) at 3745, 3690, 3628, 3600 cm^{-1}. The bands at 3745 and 3690 cm^{-1} are assigned to terminal Si-OH and Ge-OH groups, respectively [19,25]. Finally, the IR bands appearing at 3628 and 3600 cm^{-1} are assigned to acid bridging Al-OH-T(IV) groups (T(IV) = Ge or Si), since they disappear upon pyridine adsorption (middle spectrum of Fig. 8a), being observed in the difference spectrum (bottom spectrum of Fig. 8a). The presence of two

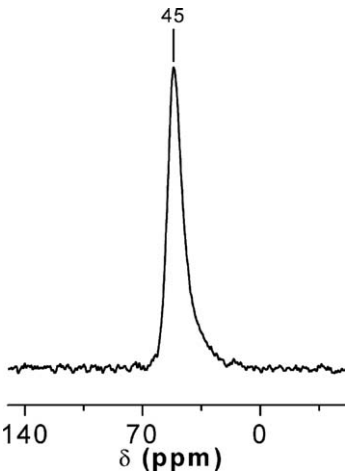

Fig. 7. ^{27}Al-MAS-NMR spectrum of an as-made Al-Ge-ITQ-7 (SiGe = 6, T(IV)/Al = 49).

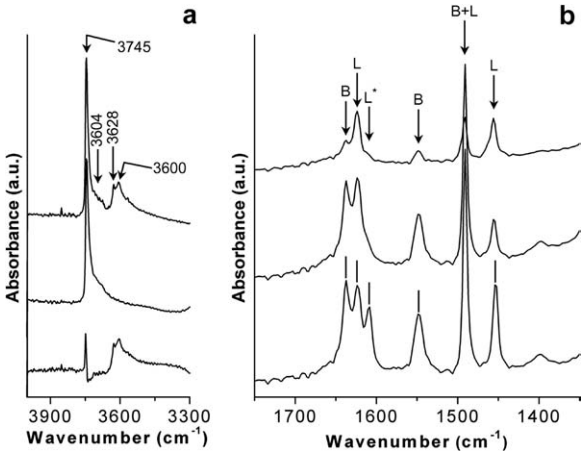

Fig. 8. Acid properties of Al-Ge-ITQ-7 zeolite (Si/Ge = 11; T(IV)/Al = 74) measured by pyridine adsorption/stepwise desorption at different temperatures. (**a**) Stretching hydroxyl region. From top to the bottom. IR spectrum upon thermal treatment at 400 °C under vacuum. After adsorbing pyridine followed by desorption at 150 °C. The differential spectrum. (**b**) Stretching C–C region of the adsorbed pyridine upon desorption at (from bottom to top) 150, 250 and 350 °C.

bands in Al-Ge-ITQ-7 associated to acid hydroxyl groups was previously observed and attributed, by means of theoretical calculations, to the presence of Al placed at different crystallographic sites [26].

The stretching C–C region of the chemisorbed pyridine on Al-ITQ-7 zeolite is shown in Fig. 8b. Pyridine adsorbed on Brönsted sites (pyridinium cations PyH$^+$) results in the presence of IR bands at 1548 and 1637 cm^{-1} (marked as B in Fig. 8b), while bands due to pyridine on Lewis sites are observed at 1623 and 1452 cm^{-1} (marked as L in Fig. 8b). An intense band at 1491 cm^{-1} is assigned to pyridine on both Brönsted and Lewis acid sites [27]. Additionally to these bands, in the spectrum obtained upon pyridine desorption at the lowest temperature (150 °C), there is a band at 1608 cm^{-1}. Therefore, we attribute this band to the presence of pyridine coordinated to germanium species, which could act as weak Lewis acid sites. This assignation is further supported by the fact that the bands at 1608, 1491 and 1452 cm^{-1} are observed in the spectrum of a Ge-ITQ-7 prepared in the absence of aluminium (Fig. 9).

To our knowledge, this is the first report on the presence of Lewis acidity on Ge-containing zeolites and could open possibilities for carrying out catalytic reactions that need of weak Lewis acid sites.

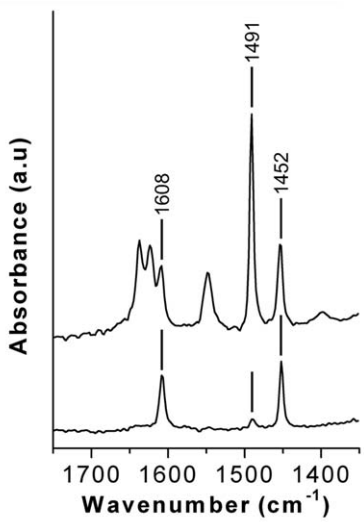

Fig. 9. IR spectra of adsorbed pyridine and desorbed at 150 °C on Al-Ge-ITQ-7 (top) and Ge-ITQ-7 (bottom) zeolites.

The temperature dependant desorption profile of pyridine on Al-ITQ-7 zeolite (Fig. 8b) indicates that a large fraction of the acid sites possesses a medium acid strength and some with stronger acidity as deduced by the IR band at 1548 cm^{-1} at 250 °C desorption temperature, and the fact that even a small number of Brönsted acid centres are able to retain pyridine at 350 °C indicating its high acid strength. On the other hand, Lewis sites associated with the presence of Ge (1608 cm^{-1}) are very weak, able to retain pyridine only at the lowest temperature. While Lewis sites, due to the presence of Aluminium in extra framework positions (1623 cm^{-1}), posses a strong acidity, since pyridine remains adsorbed at 350 °C.

Finally, the effect of the Al content in the acid properties of the Ge-ITQ-7 zeolites has been studied. The IR spectra of retained pyridine upon desorption at 150 °C on Ge-ITQ-7 samples with different Al content is shown in Fig. 10. There, it is observed that both the concentration of Brönsted and Lewis acids increases as the Al content does. The increase of the concentration of Brönsted sites can be taken as a further confirmation of the isomorphic substitution of Al in the ITQ-7 structure (Fig. 10).

4. Conclusions

Here, we have described a new and convenient synthesis procedure for the preparation of ITQ-7 within a wide range of composition based on the use of *N*-butyl-*N*-cyclohexyl-pyrrolidium cation as SDA. By following this new synthetic approach, pure silica and Al containing ITQ-7 zeolites have been obtained. These results have relevance since the earliest SDA [1] was not longer commercially available and another synthesis method does not allow to synthesise this structure in the pure silica form [2]. The characterisation results indicate that Ge and Al are isomorphically incorporated in framework sites, providing to the final solid with Lewis and Brönsted acid properties, respectively. Also, it has been found that Ge selectively occupies the T-sites at D4R units of the ITQ-7 structure.

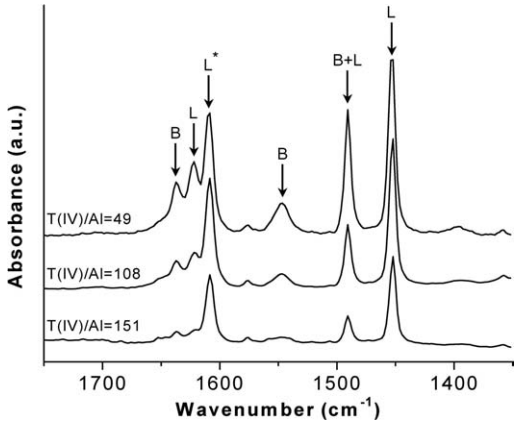

Fig. 10. IR spectra of adsorbed pyridine and desorbed at 150 °C on Al-Ge-ITQ-7 zeolites with different Al content.

Acknowledgements

The authors thank to the Spanish CICYT (Projects MAT2003-07945-C02-01 and MAT2003-07769-C02-01) for financial support. Also, funding from Generalitat Valenciana (GV01-492) is gratefully acknowledged.

References

[1] L.A. Villaescusa, P.A. Barrett, M.A. Camblor, Angew. Chem. Int. Ed. Engl. 38 (1999) 1997.
[2] A. Cantín, A. Corma, M.J. Díaz-Cabañas, F. Rey, G. Sastre, in: E. van Steel, L. Callanan, M. Claeys (Eds.), Conf. Proc. 14th Int. Zeolite Conf., Cape Town, South Africa, 2004.
[3] A. Corma, M.T. Navarro, F. Rey, J. Rius, S. Valencia, Angew. Chem. Int. Ed. Engl. 40 (2001) 2277.

[4] G. Sastre, A. Vidal-Moya, T. Blasco, J. Rius, J.L. Jorda, M.T. Navarro, F. Rey, A. Corma, Angew. Chem. Int. Ed. Engl. 41 (2002) 4722.
[5] A. Corma, M.J. Díaz-Cabañas, J. Martínez-Triguero, F. Rey, J. Rius, Nature 418 (2002) 514.
[6] M.J. Díaz-Cabañas, L.A. Villaescusa, M.A. Camblor, Chem. Commun. (Is9) (2000) 761.
[7] A. Corma, M.J. Díaz-Cabañas, V. Fornés, Angew. Chem. Int. Ed. Engl. 39 (2000) 2346.
[8] R. Lobo, M.E. Davis, Micropor. Mater. 3 (1994) 81.
[9] A. Corma, M.J. Díaz-Cabañas, M.E. Domine, F. Rey, Chem. Commun. (Is18) (2000) 1725.
[10] P. Botella, A. Corma, G. Sastre, J. Catal. 197 (2001) 81.
[11] A. Corma, J. Martínez-Triguero, C. Martínez, J. Catal. 197 (2001) 151.
[12] A. Corma, V.I. Costa-Vaya, M.J. Díaz-Cabañas, F.J. Llopis, J. Catal. 207 (2002) 46.
[13] A. Corma, A.E. Palomares, J.G. Prato, Abstract papers, Am. Chem. Soc. (2001), 221st CATL-024.
[14] T. Blasco, A. Corma, M.J. Díaz-Cabañas, F. Rey, J.A. Vidal-Moya, C.M. Zicovich-Wilson, J. Phys. Chem. 106 (2002) 2634.
[15] R.M. Barrer, in: Hydrothermal Chemistry of Zeolites, Academic Press, London, 1982, p. 174.
[16] A. Corma, I. Giménez, S. Leiva, F. Rey, M.J. Sabater, G. Sastre, S. Valencia, in: E, van Steel, L. Callanan, M. Claeys (Eds.), Conf. Proc. 14th Int. Zeolite Conf., Cape Town, South Africa, 2004.
[17] Web page of International Zeolite Association-Structure commission (http\\www.iza-structure.org).
[18] L.A. Villaescusa, Ph.D. Thesis, Universidad Politécnica de Valencia, 1999.
[19] H. Kosslick, V.A. Tuan, R. Fricke, C. Peuker, W. Pilz, W. Storek, J. Phys. Chem. 97 (1993) 5678.
[20] Y. Wang, J. Song, H. Gies, Solid-State Sci. 5 (2003) 1421.
[21] J.A. Vidal-Moya, T. Blasco, A. Corma, F. Rey, M. Puche, Chem. Mater. 15 (2003) 3962.
[22] J.A. Vidal-Moya, Ph D Thesis, Universidad Politécnica de Valencia, 2004.
[23] P. Caullet, J.L. Guth, J. Hazm, L.M. Lamblin, H. Gies, Eur. J. Solid-State Inorg. Chem. 28 (1991) 35.
[24] J.M. Thomas, J. Klinowski, Adv. Catal. 33 (1985) 199.
[25] R.K. Iler, The Chemistry of Silica, Solubility, in: Polymerization, Colloid and Surface Properties, and Biochemistry, Wiley, New York, 1979, p. 634.
[26] G. Sastre, V. Fornés, A. Corma, J. Phys. Chem. B 106 (2003) 701.
[27] C.A. Emeis, J. Catal. 141 (1993) 347.